

Where is the photospheric emission in GRBs ?

Romain Hascoët

E-mail: hascoet@iap.fr

Frédéric Daigne*

Robert Mochkovitch

UPMC-CNRS, UMR7095, Institut d'Astrophysique de Paris, F-75014, Paris, France

In the standard version of the GRB fireball model, the initial energy content of the flow is essentially thermal. However the absence of bright thermal components in most observed GRB spectra seems in contradiction with this simple picture. A first solution investigated by several authors considers additional dissipative mechanisms (e.g. [1, 2]), which results in a modified, Band-like, spectral shape of the photospheric emission. Here we investigate an alternative scenario where the GRB flow is initially magnetically dominated but contains a subdominant thermal component. The thermal component cools passively up to the photosphere, where it is radiated. We compute the resulting thermal emission and we consistently superimpose a non-thermal contribution produced either by internal shocks or by magnetic dissipation, depending on the remaining magnetization of the jet after acceleration. Within this picture, we explore the parameter space and compare model predictions (light-curves and spectra) to different tentative detections of thermal components in GRB spectra (e.g. the recent Fermi bursts 090902B, [3], and 100724B, [4]).

*Gamma-Ray Bursts 2012 Conference -GRB2012,
May 07-11, 2012
Munich, Germany*

*Institut Universitaire de France

1. Short description of the model

Photospheric emission. We consider a scenario where the flow that emerges from the central engine is accelerated by the combined effects of the magnetic field and thermal pressure. The total power of the flow \dot{E} is injected close to the central source through a geometrical section $S_0 = \pi \ell^2$, with a fraction ε_{Th} in thermal form. We also assume that the outflow becomes rapidly collimated in a cone of half opening angle θ . Following these assumptions, the initial temperature of the flow is given by

$$T_0 \simeq 0.7 \varepsilon_{\text{th}}^{1/4} \theta_{-1}^{1/2} \dot{E}_{\text{iso},53}^{1/4} \ell_7^{-1/2} \text{ MeV}, \quad (1.1)$$

where $\dot{E}_{\text{iso}} = (4/\theta^2)\dot{E}$. From mass and entropy¹ conservation during the expansion of the flow, we have

$$\beta \Gamma T^3 S = Cst, \quad (1.2)$$

where S the surface perpendicular to the flow, $\beta = v/c$ and $\Gamma = (1 - \beta^2)^{-1/2}$. With $S(R) = \pi \theta^2 R^2$ and assuming that $\beta \sim 1$ already close to the origin, we get the photospheric temperature (source frame)

$$T_{\text{ph}} = T_0 \times \left(\theta^{-2/3} R_{\text{ph}}^{-2/3} \ell^{2/3} \Gamma_{\text{ph}}^{-2/3} \right) \quad (1.3)$$

and luminosity

$$L_{\text{ph}} = \Gamma_{\text{ph}}^2 a T^4(R_{\text{ph}}) c \times S(R_{\text{ph}}) = \dot{E}_{\text{th}} \times \left(\theta^{-2/3} R_{\text{ph}}^{-2/3} \ell^{2/3} \Gamma_{\text{ph}}^{2/3} \right), \quad (1.4)$$

where R_{ph} and Γ_{ph} are the radius and Lorentz factor at the photosphere. To estimate the photospheric radius we assume that most of the acceleration is completed at the photosphere² (see e.g. [5, 6]) giving

$$R_{\text{ph}} \simeq \frac{\kappa \dot{M}}{8\pi c \Gamma^2} = \frac{\kappa \dot{E}_{\text{iso}}}{(1 + \sigma) 8\pi c^3 \Gamma^3} \simeq 2.7 10^{12} \frac{\kappa_{0.2} \dot{E}_{\text{iso},52}}{(1 + \sigma) \Gamma_2^3} \text{ cm} \quad (1.5)$$

where κ is the material opacity and σ the remaining magnetization in the flow at the end of acceleration so that $\dot{E}/(1 + \sigma)$ is the injected kinetic power. In the following, the photospheric emission is qualified as 'thermal'. However, we take into account the spectral broadening due to the complex geometry of the photosphere (see e.g. [7]) leading to a non-Planckian spectrum.

Non thermal emission. As for the prompt non thermal emission, we consider two possibilities.

- If the remaining magnetization is low ($\sigma \ll 1$) the kinetic energy of the outflow can be extracted by internal shocks. Using the multiple-shell model of [8], we can consistently superimpose the light-curves and spectra of the thermal (released at the photosphere) and non thermal (produced by internal shocks) emissions. An example of synthetic burst is presented in figure 1.
- If the remaining magnetization is high, internal shocks are inhibited and the magnetic energy can be released via reconnection. A detailed modeling of the reconnection process is not yet available to compute light-curves. We simply assume that a fraction f_{Nth} of the outflow energy is converted into non thermal radiation and that the associated spectrum has a Band function shape, with a peak energy fixed by the Amati relation. A sequence of synthetic spectra obtained following this prescription is presented in figure 2.

¹We assume that no dissipation takes place below the photosphere.

²In Hascoet et al. (in preparation) we also discuss the case where the acceleration is incomplete at the photosphere.

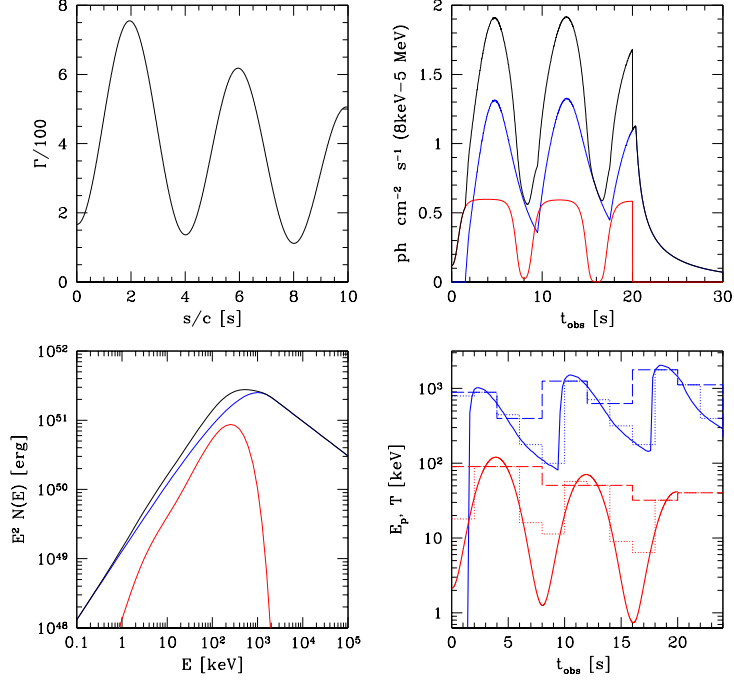


Figure 1: Thermal and non thermal emission from a variable outflow – internal shock framework. *Top left:* initial distribution of the Lorentz factor in the outflow. *Top right:* thermal (red), non-thermal (blue) and total (black) photon flux in the 8 keV - 5 MeV spectral range. *Bottom left:* thermal (red), non-thermal (blue), and total (black) time-integrated spectra. *Bottom right:* instant temperature (red) of the thermal emission and instant peak energy (blue) of the non-thermal emission (source frame). The adopted flow parameters are $\dot{E}_{\text{iso}} = 10^{53} \text{ erg.s}^{-1}$, $\epsilon_{\text{th}} = 0.03$, $\sigma = 0.1$, $\ell = 3 \cdot 10^6 \text{ cm}$ and $\theta = 0.1 \text{ rd}$; a redshift $z = 1$ is assumed. The binned curves represent the peak energy and temperature that would be measured by an observer from spectra integrated on bins with a resolution of 2 s (dashed dotted lines) and 4 s (dashed lines).

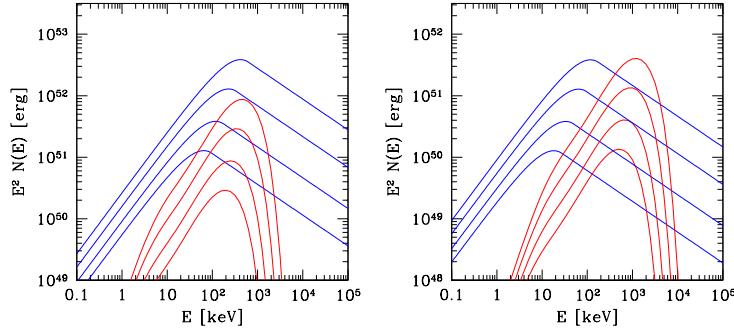


Figure 2: Thermal and non thermal emission from a variable outflow – magnetic reconnection framework. The Lorentz factor distribution adopted for the calculation of the thermal emission is the same as in figure 1. The non thermal spectrum is simply parametrized by a Band function, with its peak energy fixed by the Amati relation. In each panel there is a sequence of thermal (red) and non-thermal spectra calculated for four values of ϵ_{th} and f_{Nth} : 0.01, 0.03, 0.10 and 0.30. *Left:* spectra obtained for an isotropic power $\dot{E}_{\text{iso}} = 10^{53} \text{ erg s}^{-1}$. *Right:* spectra obtained for an isotropic power $\dot{E}_{\text{iso}} = 10^{52} \text{ erg s}^{-1}$.

2. Discussion

Even if the acceleration of the relativistic outflow is driven by a magnetic process, it is likely that a subdominant thermal component is also injected from the central engine. In this framework we compute the expected non thermal and thermal emissions and obtain the following results :

- The level of the thermal emission relative to the non thermal one can vary over a wide range depending on the physical properties (mainly the Lorentz factor and energy content) of the ultra-relativistic outflow. Depending on the remaining magnetization at the end of acceleration, the non thermal emission is expected to be produced by internal shocks (low σ , low efficiency mechanism) or magnetic reconnection (high σ , high efficiency mechanism ?).
- If recent tentative detections of thermal emission were to be confirmed (e.g. GRB 100724B, Guiriec et al. 2011; see also McGlynn et al., these proceedings) this would indicate that the thermal component of the outflow is subdominant ($\epsilon_{\text{th}} \ll 1$).
- A few peculiar GRBs (e.g. GRB 090902B, [3]) may show that the thermal component can sometimes be dominant, favoring a thermal acceleration scenario in these rare cases.
- Finally it is interesting to note that in the internal shock framework, the temperature (along with the flux) of the thermal emission is expected to vary over a wide range (typically two decades) because of the Lorentz factor variations. These variations of the observed temperature are however partially smoothed out as they occur on a variability timescale which is usually smaller than the integration time for the spectral analysis (see figure 1). Moderate variations of the temperature are indeed observed in GRB 100724B [4], in agreement with the scenario where internal shocks are the main dissipation mechanism. A detailed comparison is in progress.

The current tentative detections of the photospheric emission clearly represent a promising diagnostic to shed light on the nature of the GRB relativistic outflows and dissipating mechanisms during the prompt phase.

References

- [1] M. J. Rees, and P. Mészáros, *Dissipative Photosphere Models of Gamma-Ray Bursts and X-Ray Flashes*, *ApJ*, **628** (2005) 468 [astro-ph/0412702].
- [2] A. M. Beloborodov, *Collisional mechanism for gamma-ray burst emission*, *MNRAS*, **407** (2010) 1033 [astro-ph/0907.0732].
- [3] A. A. Abdo, A. Ackermann, M. Ajello, et al., *Fermi Observations of GRB 090902B: A Distinct Spectral Component in the Prompt and Delayed Emission*, *ApJL*, **706** (2009) L138 [astro-ph/0909.2470].
- [4] S. Guiriec, V. Connaughton, M. S. Briggs, et al., *Detection of a Thermal Spectral Component in the Prompt Emission of GRB 100724B*, *ApJL*, **727** (2011) L33 [astro-ph/1010.4601].
- [5] A. Tchekhovskoy, R. Narayan, J. C. McKinney, *Magnetohydrodynamic simulations of gamma-ray burst jets: Beyond the progenitor star*, *New Astronomy*, **15** (2010) 749 [astro-ph/0909.0011].
- [6] J. Granot, *The effects of sub-shells in highly magnetized relativistic flows*, *MNRAS*, **421** (2012) 2467 [astro-ph/1109.5315].
- [7] J. Goodman, *Are gamma-ray bursts optically thick ?*, *ApJ* **308** (1986) L47.
- [8] F. Daigne, and R. Mochkovitch, *Gamma-ray bursts from internal shocks in a relativistic wind: temporal and spectral properties*, *MNRAS* **296** (1998) 275 [astro-ph/9801245].